

The Influence of Ram Pressure on the Evolution of Tidal Dwarf Galaxies

R. Smith^{1*}, P. A. Duc², G. N. Candlish¹, M. Fellhauer¹, Y. K. Sheen¹, B. K. Gibson³

¹*Departamento de Astronomía, Universidad de Concepción, Casilla 160-C, Concepción, Chile*

²*Laboratoire AIM, Service d'astrophysique, CEA Saclay, Orme de Merisiers, Batiment 709, 91191 Gif sur Yvette cedex, France*

³*Jeremiah Horrocks Institute, University of Central Lancashire, Preston, PR1 2HE, United Kingdom*

11 June 2021

ABSTRACT

The formation mechanism of tidal dwarf galaxies means they are expected to contain little or no dark matter. As such, they might be expected to be very sensitive to their environment. We investigate the impact of ram pressure on tidal dwarf galaxies in a parameter study, varying dwarf galaxy properties and ram pressures. We submit model tidal dwarf galaxies to wind-tunnel style tests using a toy ram pressure model. The effects of ram pressure are found to be substantial. If tidal dwarf galaxies have their gas stripped, they may be completely destroyed. Ram pressure drag causes acceleration of our dwarf galaxy models, and this further enhances stellar losses. The dragging can also cause stars to lie in a low surface brightness stellar stream that points in the opposite direction to the stripped gas, in a manner distinctive from tidal streams. We investigate the effects of ram pressure on surface density profiles, the dynamics of the stars, and discuss the consequences for dynamical mass measurements.

Key words: methods: N-body simulations — galaxies: clusters: general — galaxies: evolution — galaxies: kinematics and dynamics — galaxies: intergalactic medium

1 INTRODUCTION

Tidal dwarf galaxies (TDGs) are, by definition, bound structures formed from tidal tails of gas and stars (Duc 2012). The tidal tails are produced by tides or gravitational torques when progenitor galaxies merge or gravitationally interact. In the nearby Universe, the progenitors are typically two late-type galaxies, whereas TDG formation about early type galaxies is very rare (Kaviraj et al. 2012). There are at least two mechanisms that can form substructures within tidal tails with masses equal to dwarf galaxies ($\sim 10^7 - 10^9 M_{\odot}$). The first is collapse through Jeans instabilities – when an object has sufficient mass to overcome internal support provided by pressure, and collapses to form a self-bound object (Barnes & Hernquist 1992). Wetzstein et al. (2007) find that the presence of gas is required for TDGs to form in this manner. The result is numerous star-forming gas clumps distributed along a tidal tail. The second is where a large region of the outer disk material tends to pool at the end of a tidal tail, and becomes self-bound (Elmegreen et al. 1993). This second formation mechanism tends to produce a single, massive, TDG. Simulations have demonstrated that this type of TDG forms more readily when the progenitor galaxies have large, extended, dark matter halos. If they

did not, numerous, low mass, ‘beads-on-a-string’ tend to form (Bournaud et al. 2003; Duc et al. 2004). In fact, observed TDGs appear to either form large numbers of low mass galaxies, or a single massive object (Knierman et al. 2003).

While TDGs remain associated with their natal tidal tails, they are easily identified. However with sufficient time, some TDGs may no longer be seen in close proximity to tidal features. Such TDGs may be difficult to differentiate from more ‘typical’ dwarf irregulars (dIrrs), as they have similar luminosities, morphologies, gas fractions, and sizes (Hunter 1997; Duc 2012). A number of possible approaches to identify long-lived TDGs are compared and discussed in Hunter et al. (2000) and Duc (2012). As TDGs are formed from the recycled gas of more massive (and metal-rich) progenitors, they are expected to show elevated metallicities compared to other star forming dwarfs of similar luminosity. Even when TDGs form in the very outskirts of the progenitor galaxies, their metallicity remains high (Weilbacher et al. 2003), perhaps due to strong radial mixing during mergers (Di Matteo et al. 2011). A comparison of the dispersion, skewness, and kurtosis of the metallicity distribution functions of putative TDGs, as opposed to dark matter-dominated dwarfs, may prove invaluable as a tool to

* E-mail: rsmith@astro-udec.cl

discriminate between these competing scenarios¹. Another clue may come from the spectral energy distribution of star forming regions in TDGs, as they may be forming their first generation of stars but, at the same time, be chemically evolved (Boquien et al. 2010).

A clear distinction between typical dIrrs and TDGs lies in their dark matter content. TDGs should contain little or no dark matter (Bournaud 2010). This may be detectable in the behaviour of their rotation curves, or in terms of a deviation from the Tully-Fisher relationship of normal, dark matter-dominated, dwarfs (Hunter et al. 2000). For a few TDGs, the mass budget has been measured in terms of the total stellar, atomic, and molecular gas detected; in those cases, a small amount of additional ‘missing’ mass, not accounted for in this detected mass budget, is required in order to explain the internal dynamics, under the assumption of dynamical equilibrium. Explanations include the presence of ‘dark gas’ (Bournaud 2010) or modified Newtonian dynamics (Boquien et al. 2010).

The lack of a protective dark matter halo could cause TDGs to be extremely sensitive to their environment. In the absence of resonant stripping (Muccione & Ciotti 2004; D’Onghia et al. 2009), dwarf galaxies which initially have massive dark matter halos are protected from stellar mass loss due to external tides, until ~80-90% of their dark matter has been stripped (Knebe et al. 2006; Peñarrubia et al. 2008; Smith et al. 2013). Therefore, TDGs which have no dark matter from the beginning, should be susceptible to tidally induced mass loss. Damaging tides could initially arise from the gravity of the progenitor galaxies. Simulations suggest a fraction of the initially formed TDGs can survive tidal destruction from their progenitors in order to become long-lived TDGs (Bournaud et al. 2003; Bournaud 2010). TDGs that survive this first hurdle and, additionally, avoid infalling back onto their progenitors, must face the tides of the group or cluster environment in which they find themselves.

Besides tides, TDGs may also be susceptible to ram pressure stripping. The effects of ram pressure on the behaviour of the stars of a galaxy is generally assumed to be very minor in giant late-type galaxies. This is because the cross-sectional area of stars and molecular clouds is too small to feel any significant acceleration directly from the hot gas that causes ram pressure. However, the removal of this gas can lower the overall disk mass. This may result in some thickening of the stellar disk (Farouki & Shapiro 1980). However, this is generally assumed to be minor as the gas fraction is typically low (~10%) in nearby giant late-type disk galaxies (Gavazzi et al. 2008).

At lower masses, however, late-type dwarf galaxies can contain very high gas fractions, with several times more gas than stars (Gavazzi et al. 2008). In such galaxies, the removal of the gas mass changes significantly the galaxy’s potential, causing thickening of the stellar disk by roughly a factor of two (Smith et al. 2012).

In fact, the effect of ram pressure on the stars goes beyond disk thickening. In Schulz & Struck (2001), it was noted that the stellar disc of their models was displaced several kiloparsecs downwind, in their ram pressure simulations. This effect was further studied by Smith et al. (2012) using simulated late-type dwarf galaxies embedded in dark matter halos. Although the stars alone cannot feel directly the ram pressure, the gas disc presents a cross-sectional area A to the ram pressure wind. As such, it feels a drag force ($F_{\text{drag}} = A \times P_{\text{ram}}$ where P_{ram} is the ram pressure) and is thus accelerated in the direction of the ram pressure wind. Meanwhile, the gravitational attraction between the stars and the gas disk causes the drag force felt by the gas disk to be shared with the stellar disk. In fact, the effect is not limited to the stars - the central dark matter surrounding the gas disk also feels the drag force. The net result is displacement of the gas and stellar disk, and central dark matter, downwind of the ram pressure by several kiloparsecs with respect to the outer halo. The process is referred to as *ram pressure drag*. Smith et al. (2012) also noted that, because the stellar disk is gravitationally dragged by its centre, a short-lived (<200 Myr) conical-like distortion of the disk results. This is because the stellar disk centre is displaced preferentially with respect to the outer stellar disk.

The effects of ram pressure drag on TDGs are expected to be even more substantial. Like normal late-type dwarfs, TDGs appear to have very high gas fractions (Duc et al. 2000; Hibbard et al. 2001; Bournaud et al. 2004; Mundell et al. 2004; Neff et al. 2005; Bournaud et al. 2007; Koribalski & López-Sánchez 2009; Bournaud 2010). However, unlike normal late-type dwarfs, TDGs contain little or no dark matter. Therefore the loss of the gas potential when the gas is stripped should result in stronger disk thickening in TDGs than was seen in our dIrr models (Smith et al. 2012). Also, in normal late-type dwarfs, the ram pressure drag force must tow the mass of the stars and dark matter, whereas in a TDG it need only tow the mass of the stars. Therefore, for the same momentum transfer from the ram pressure wind, a TDG should have a greater acceleration.

If TDGs are indeed as sensitive to their environment as proposed, then we might expect to see some indication of this in their observed properties. Kaviraj et al. (2012) note that the majority of their TDGs are located in the field environment. Sheen et al. (2009) detect TDGs in the Coma cluster, but specifically in the cluster outskirts. This perhaps suggests that the cluster environment is a harsh environment for TDGs, but it could also suggest that the high interaction velocities of cluster galaxies are not conducive in creating the tidal tails from which TDGs form. If the latter, then TDGs may form outside the cluster environment, and then be subsequently accreted into the cluster. Possible examples include ARP 105 (Duc & Mirabel 1994), NGC 5291 (Duc & Mirabel 1998), IC 1182 (Iglesias-Páramo et al. 2003), and VCC 2062 (Duc et al. 2007). However a dense environment where galaxy relative velocities are lower than in clusters (i.e., compact groups) may be highly conducive to TDG formation. Temporin et al. (2003) find the compact group CG J1720-67.8 is rich with TDG candidates. From a sample of 42 Hickson compact groups, Hunsberger et al. (1996) state that perhaps as many as half of all the dwarfs in their compact groups are TDGs.

¹ For example, dwarf galaxy IKN in the M81 group, a potential TDG candidate (Lianou et al. 2010), possesses a negative skewness somewhat in excess of the other dwarf spheroidals in the group; whether this is indicative of a fundamental difference, or simply a coincidence, should be assessed, using the tools of, say, Pilkington et al. (2012).

Numerical simulations have provided a powerful tool in studying the formation mechanisms of TDGs (e.g., Barnes & Hernquist 1992; Elmegreen et al. 1993; Bournaud et al. 2003; Duc et al. 2004; Wetzstein et al. 2007). They have also been used to model dynamics in individual, well-studied, interacting systems (Duc et al. 2000; Struck et al. 2005; Hancock et al. 2007). Recchi et al. (2007) use 2D chemo-dynamical models to understand how TDGs react to the feedback from ongoing star formation, and find that star formation can continue for more than 300 Myr. In high-resolution cluster formation simulations, Puchwein et al. (2010) finds that up to $\sim 30\%$ of their intra-cluster stars are formed extra-galactically in stripped gas clouds. With increasing resolution, it has recently become possible to better study the properties of TDGs formed in galaxy interaction/merger simulations such as mass, internal dynamics, or even rotation curves (Bournaud et al. 2008).

Here we use numerical simulations to study the response of model TDG galaxies to gas removal by ram pressure stripping, and ram pressure drag. Even if TDGs form outside the cluster, they may later be accreted into the cluster. These TDGs will then be subjected to ram pressure from their motion through the intracluster medium. However ram pressure is not limited to occurring in the cluster environment. Although the densities of the hot gas appear lower (Mushotzky 2004), dwarf galaxies moving through the *intra-group* medium may also suffer ram pressure (Marcolini et al. 2003). In fact, even individual galaxies contain their own hot gaseous halos that may exert ram pressure on other galaxies that move through them. A hot gaseous halo is seen surrounding the Milky Way (Bregman & Lloyd-Davies 2007; Lehner et al. 2011; Gupta et al. 2012), and also in other galaxies (Tumlinson et al. 2011; Tripp et al. 2011). Ram pressure from the Milky Way’s (MW’s) hot gaseous halo has been used to explain the morphology-density relation of dwarf galaxies surrounding the MW (Mayer 2005). Recently the argument was reversed in Gatto et al. (2013). By assuming that ram pressure caused the observed halt in star formation in the dwarf spheroidals Sextans and Carina, limits were placed on the density of the hot gaseous halo of the MW. That derived density is in broad agreement with previous measurements. The presence of the MW’s hot halo is also seen indirectly through its action on the Magellanic stream (Weiner & Williams 1996; Stanimirović et al. 2002; Putman et al. 2003). The existence of hot gaseous halos is expected in the galaxy formation framework of Λ CDM (Feldmann et al. 2013), and may be an important ingredient in forming disks with more realistic morphologies (Hambleton et al. 2011; Brook et al. 2012).

To study the effects of ram pressure on TDGs, we subject TDG models to idealised wind-tunnel style ram pressure tests. The ram pressures and properties of the TDG models are varied in a parameter study. We show that the effects of ram pressure can be very significant for TDGs – in fact when their gas is stripped, they are completely destroyed. This may have some impact on the survival time of TDGs, a key ingredient in discussions regarding the fraction of dwarf galaxies of tidal origin. We describe the set up of our model galaxies, the parameter study, the numerical code, and the ram pressure model in §2. Our results are presented in §3 including baryonic mass loss, drag, stellar streams, effects on surface density profiles and stellar dynamics, and im-

plications for dynamical mass measurements in TDGs. We discuss our results in §4 and summarise the conclusions in §5.

2 SETUP

2.1 Disk galaxy models

Our tidal dwarf galaxy (TDG) models consist of two components: exponential discs of gas and stars. The methods used to form each component will be discussed briefly in the following sections. The true spatial distribution of gas and stars in TDGs is not well constrained observationally, as they are typically poorly resolved. However a disk-like distribution is a reasonable assumption, given the rotating gas disks of TDGs that are both observed (Bournaud et al. 2007), and produced in simulations (Bournaud et al. 2008).

Radially, the stellar and gas disk both have an exponential form

$$\Sigma(R) = \Sigma_0 \exp(-R/R_d) \quad (1)$$

where Σ is the surface density, Σ_0 is central surface density, R is radius within the disk, and R_d is the scale-length of the disk. For simplicity, we assume the scale-length of the stellar disk and gas disk are equal.

We distribute the particles vertically out of the disk using the form given by Spitzer’s isothermal sheet:

$$\rho(R, z) = \frac{\Sigma(R)}{2z_d} \operatorname{sech}^2(z/z_d). \quad (2)$$

Following Springel & White (1999), we make z_d a fixed fraction of the disk scalelength, and we choose $z_d = 0.1 R_d$.

Disk particles are initially set-up on circular orbits. The circular velocity of an exponential disk can be calculated from (Freeman 1970):

$$v_c^2(R) = R \frac{d\phi}{dR} = 4\pi G \Sigma_0 R_d y^2 [I_0(y)K_0(y) - I_1(y)K_1(y)] \quad (3)$$

where $y \equiv R/2R_d$, and I and K are modified Bessel functions. In practice, the term in square brackets is evaluated using a look-up table.

The Toomre stability criterion is defined as:

$$Q \equiv \frac{\kappa \sigma_R}{3.36 G \Sigma} > 1 \quad (4)$$

where Σ is the surface density, σ_R is the radial velocity dispersion, and κ is the epicyclic frequency defined, using the epicyclic approximation (Springel & White 1999). The azimuthal velocity dispersion σ_ϕ , and the velocity dispersion out of the plane of the disk σ_z , are functions of σ_R . We use $\sigma_\phi^2 = \frac{\sigma_R^2}{\gamma^2}$ where

$$\gamma^2 \equiv \frac{4}{\kappa^2 R} \frac{d\Phi}{dR}, \quad (5)$$

and $\phi_z = 0.6 \cdot \phi_R$ (Shlosman & Noguchi 1993). In practice, a radially varying velocity dispersion is chosen that satisfies $Q > 1.5$ at all radii. This ensures that disks are sufficiently stable such that their properties do not change significantly for models evolved in isolation. This velocity dispersion is physically added to the velocities of the star particles. Instead, for gas particles, a thermal energy u of the particles

is chosen that is equivalent to the required velocity dispersion σ at that radius ($u = \sigma^2/(\gamma - 1)$ where $\gamma = 5/3$ for a monatomic gas). In a final step, the rotation velocity v_ϕ of all particles in the disk is adjusted, accounting for the outwards pressure term caused by the gradient in the velocity dispersion:

$$v_\phi^2(R) = v_{\text{circ}}^2 - \frac{R}{\rho} \left| \frac{dP}{dR} \right| \quad (6)$$

where v_{circ} is the circular velocity, and other terms have their usual meaning. We note that equation 6 is strictly only valid in the plane of the disk. However, in practice, we find this simplification has negligible consequences. We evolve all of our disk models in isolation for at least 2.5 Gyr to ensure they are dynamically stable, and that any transient effects have settled. Therefore, none of our models are placed in wind-tunnel tests until they are in dynamical equilibrium. Each TDG model is composed of 1×10^5 disk particles, split equally between gas and stars.

We emphasise that we are not forming TDGs in our simulations – instead we choose to start our wind-tunnel tests with dynamically stable models. In reality, it is uncertain if real TDGs are so close to dynamical equilibrium. However we wish to examine the effects of ram pressure, alone, on the dynamics of TDGs, and it is easier to detect it on models that would otherwise be in equilibrium in the absence of ram pressure.

2.2 Tidal dwarf galaxy models – a parameter study

Our parameter study involves varying the mass, disk scale-length, and gas fraction of the TDG models. We consider two masses of TDG model: a lower mass model and a higher mass variant with a total mass of $1 \times 10^7 M_\odot$ and $1 \times 10^8 M_\odot$, respectively. We consider three disk sizes with effective radii of 1, 2, or 3 kpc, typical of that observed in both young and evolved TDGs (Paudel 2013; in prep). As TDGs are observed to be typically gas-rich, we consider three gas fractions: 50% (equal gas and stars), 70%, and 90% (very gas-rich).

We subject each model TDG to wind tunnel tests with a fixed wind speed. However, we vary the wind speed between the tests, in order to quantify a TDG model’s response to differing ram pressures. We consider a sufficient range of ram pressure to ensure that each model is entirely stripped of its gas when subjected to the uppermost wind speed.

When describing a specific model, we use a shorthand label. For example M8gf50R1 is the model with total mass of $10^8 M_\odot$ (M8), with a gas fraction (gf50) of 50%, and with an effective radius (R1) of 1 kpc. A list of the key properties of each model TDG, and the wind speeds to which they were subjected, can be found in Table 1.

2.3 The Code

In this study we use GF (Williams & Nelson 2001; Williams 1998), a gravitational Tree N-body + SPH code that operates primarily using the techniques described in Hernquist & Katz (1989). While the Tree code allows for rapid calculation of gravitational accelerations, the SPH code allows us to include an HI gas component to our

tidal dwarf galaxy models. In all simulations, the gravitational softening length, ϵ , is fixed for all particles at a value of 100 pc. Gravitational accelerations are evaluated to quadrupole order, using an opening angle $\theta_c=0.7$. A second-order individual particle time-step scheme was utilised to improve efficiency following the methodology of Hernquist & Katz (1989). Each particle was assigned a timestep that is a power of two division of the simulation block timestep, with a minimum timestep of ~ 5 yr. Assignment of timesteps for collisionless particles is controlled by the criteria of Katz (1991), whereas SPH particle timesteps are assigned using the minimum of the gravitational timestep and the SPH Courant conditions with a Courant constant $C=0.1$ (Hernquist & Katz 1989).

As discussed in Williams et al. (2004), the kernel radius h of each SPH particle was allowed to vary such that at all times it maintains between 30 and 40 neighbours within $2h$. In order to realistically simulate shocks within the SPH model, the artificial viscosity prescription of Gingold & Monaghan (1983) is used with viscosity parameters $(\alpha, \beta) = (1, 2)$. The equation of state for the gas component of the galaxies is adiabatic. We choose a velocity dispersion that varies radially within the disk, such that the Toomre stability criteria (Eqn. 4) is satisfied at all radii. For example, for Model M8gf70R1 this requires a velocity dispersion of 12 km s^{-1} in the disk centre, falling to 5 km s^{-1} in the outer disk. This is in good agreement with the observed radial variation in HI velocity dispersion in late-type disks (Tamburro et al. 2009; Pilkington et al. 2011). We do not include star formation in these models, although we note that stellar feedback may further enhance gas stripping by ram pressure (Gatto et al. 2013). Our choice of an adiabatic equation of state aids us in setting up stable disks. Thus, our models are dynamically stable before they are subjected to the effects of ram pressure. In this way, we can clearly identify the effects of ram pressure on galaxy stability when we subject them to a wind tunnel test. Although our simplifying choice of an adiabatic equation of state is a gross simplification of a real galaxy’s ISM, all of our key results occur primarily because of the removal of the gas mass by ram pressure. With this in mind, we do not expect that any of our key results would change significantly if we had instead used a more complex (and numerically expensive) treatment for the ISM, as long as the mass of the ISM that is removed by ram pressure is comparable. Tonnesen & Bryan (2009) conduct high resolution simulations of disk galaxies undergoing ram pressure in which a multiphase ISM is resolved. To first order, the mass of gas stripped from their models does not depend sensitively on their ability to resolve a complex multiphase ISM.

2.4 The Ram Pressure Model

The ram pressure stripping model is very similar to that presented in Vollmer et al. (2001) and is the same as the model employed in Smith et al. (2012). In this model, additional acceleration vectors are added to individual gas particles to mimic the ram pressure. A live intra-cluster medium (ICM) component is not included. For an individual gas cloud, moving through the ICM of density ρ_{ICM} , with a velocity v , the pressure on its surface due to sweeping through the medium

Galaxy model	Total mass (M_{\odot})	Gas fraction	Effective radius (kpc)	Central surface density ($M_{\odot} \text{ pc}^{-2}$)	Wind speeds* (km s^{-1})
M8gf50R1	10^8	0.5	1.0	15.9	200,400,800
M8gf70R1	10^8	0.7	1.0	15.9	200,400,800
M8gf90R1	10^8	0.9	1.0	15.9	200,400,800
M8gf50R2	10^8	0.5	2.0	4.0	200,400,600
M8gf70R2	10^8	0.7	2.0	4.0	200,400,600
M8gf90R2	10^8	0.9	2.0	4.0	200,400,600
M8gf50R3	10^8	0.5	3.0	1.8	100,200,300
M7gf70R1	10^7	0.7	1.0	1.6	100,200,300,400

Table 1. Main properties of the model tidal dwarf galaxies (columns 1-5) and wind-tunnel tests conducted upon them (column 6). (*In the frame of reference of the TDG, ram pressure occurs from incoming wind of hot gas. The quoted velocities are for a ram pressure wind with densities typical of the outer Virgo cluster, loose galaxy groups, or the inner Milky Way halo.)

is assumed to be

$$P_{\text{ram}} = \rho_{\text{ICM}} v^2 \quad (7)$$

In order to calculate the strength of the acceleration that gas clouds will feel as a result of ram pressure, we follow Vollmer et al. (2001). A constant column density is assumed for each individual cloud. This has the advantage that the acceleration due to ram pressure is the same for all clouds, disregarding their masses. A value of $\Sigma_{\text{cld}} = 7.5 \times 10^{20} \text{ cm}^{-2}$ ($\sim 6.0 M_{\odot} \text{ pc}^{-2}$) is used. This is comparable with measurements made by Rots et al. (1990) and Crosthwaite et al. (2000) on nearby face-on galaxies. The acceleration due to ram pressure can therefore be written as

$$a_{\text{ram}} = \frac{P_{\text{ram}}}{m_{\text{H}} \Sigma_{\text{cld}}} \quad (8)$$

where m_{H} is the mass of a hydrogen atom. In the galaxy model's frame of reference, the effect of its motion through the ICM is that of an ICM wind of velocity v and density ρ_{ICM} ; a_{ram} therefore always acts in the direction of the velocity vector of the wind.

Once more, following Vollmer et al. (2001), a shading criteria is used to select gas particles that feel the influence of ram pressure, and gas particles that are shielded by other gas particles upstream in the wind. In the simulation, gas particles are point particles and therefore have no cross-section by which to shield other particles. However, we can calculate a particle's cloud radius r_{cld} if we know its mass m_{p} and once more assume it has the column density Σ_{cld} . Then $r_{\text{cld}} = [m_{\text{p}} / (\pi m_{\text{H}} \Sigma_{\text{cld}})]^{0.5}$. In practice, each particle extends an imaginary vector along the direction of motion of the galaxy's disk and checks to see if any other particles' cross-sections (πr_{cld}^2) cross the vector. If there are none, then the gas particle is unshielded and will feel the acceleration a_{ram} . In this case, an additional acceleration vector of magnitude a_{ram} is added to the particle's equation of motion, in the direction of the ICM wind.

For simplicity, we consider only the atomic gas content (HI) in our models, neglecting the presence of molecular gas (H_2), and Helium (He). As H_2 clouds have a small cross-section, they are not expected to be efficiently ram pressure stripped (Quilis et al. 2000)². Thus in effect we have neglected an unstrippable mass component that may be $\sim 20\%$

the mass of the HI and He combined (Braine et al. 2001). Including such a mass component could cause our model galaxies to respond as if they have gas fractions which are $\sim 10\text{-}15\%$ lower than stated. However this effect may be entirely cancelled by our models not including a Helium component, which means we may actually underestimate the gas mass loss by as much as 40% (Tielens 2010).

We explore models where the ram pressure wind encounters the TDG disk face-on. We do not expect our results are sensitive to this, as ram pressure is expected to affect disk galaxies in a similar manner for a wide range of wind inclination, except for near edge-on ram pressure stripping (Vollmer et al. 2001; Marcolini et al. 2003; Roediger & Brüggén 2006). We fix a constant velocity for the test galaxy and for the density of the ICM it is moving through. In the frame-of-reference of the test galaxy, it experiences an oncoming, uniform density, constant velocity wind. We refer to such tests as 'wind-tunnel' tests. It should be noted that this situation is artificial for real galaxies, in clusters or groups, or in interacting galaxies, whose orbits subject them to both changing wind velocities and densities of hot gas. However, as we will later show, some aspects of the TDGs' response to ram pressure is very complex, even in these idealised wind-tunnel tests. We will consider time-varying ram pressures in a later study.

We choose an arbitrary fixed ICM density of $\rho_{\text{ICM}} = 10^{-4} \text{ Hydrogen atoms cm}^{-3}$. For a Virgo-like ICM distributed in a Beta-model (like cluster model 'C1' of Roediger & Brüggén 2007), our choice corresponds to densities found in the outskirts of the Virgo cluster ($R \sim 1000 \text{ kpc}$). This choice of density is also a reasonable approximation for the hot gas halo of the Milky Way (Weiner & Williams 1996; Stanimirović et al. 2002; Putman et al. 2003; Bregman & Lloyd-Davies 2007; Lehner et al. 2011; Gupta et al. 2012), or loose groups of galaxies (Mushotzky 2004).

As we have fixed the ICM density, we vary the strength of ram pressure between wind tunnel tests, by choosing the wind speed v_{wind} . We subject our standard galaxy model to an ICM wind of constant velocity v_{wind} with a face-on inclination; v_{wind} is varied from 100–800 km s^{-1} . This covers typical wind-velocities of dwarf galaxies orbiting in the Milky Way (100–200 km s^{-1}), galaxies in loose groups (200–500 km s^{-1} ; Zabludoff & Mulchaey 1998), and the velocities of cluster galaxies ($\sim 800 \text{ km s}^{-1}$).

² Although see Vollmer et al. (2008) for possible stripped H_2 .

As ram pressure is proportional to the intracluster medium density times the galaxy velocity squared, the ram pressures we consider are also representative of ram pressure in denser environments (such as cluster cores), or lower density environments (such as the outer halo of the Milky Way), if we rescale the wind speeds quoted in this paper by a constant factor. For example, for cluster model ‘C1’ of Roediger & Brüggén (2007) at a radius of $r \sim 250$ kpc (near the cluster centre), the hot gas density is a factor ~ 10 times higher than our choice of ρ_{ICM} . However, equivalent ram pressures as those in this study, will occur for galaxies moving through such a medium if they have velocities $\sqrt{10} \approx 3$ times *lower* than our stated velocities. Similarly, the hot gas density in the outer hot gas halo ($r=250$ kpc) of the Milky Way is a factor ~ 10 times lower than our choice of ρ_{ICM} (Blitz & Robishaw 2000; Sembach et al. 2003), but equivalent ram pressures will occur for galaxies with velocities approximately 3 times *higher*. For a complete list of the wind-tunnel tests applied to each of the models, see Table 1.

Each model galaxy is subjected to the ICM wind for 2.5 Gyr. This duration is chosen as it allows sufficient time for gas that has been unbound to be accelerated away from the stellar disk. The duration is also physically motivated. Trentham & Tully (2002) give the crossing time of the Virgo cluster as one tenth of a Hubble time. Therefore 2.5 Gyr represents a rough timescale for which a Virgo cluster galaxy might experience ram pressure over 1-2 orbits in the cluster.

We emphasise that this model should be regarded as a toy model of ram pressure. Recent ram pressure stripping models discussed in the literature (see for example Roediger & Brüggén 2007) have advanced significantly beyond the simple ram pressure recipe of Vollmer et al. (2001). Increasingly high resolution along the ISM-ICM boundary has allowed quantification of additional stripping mechanisms such as Rayleigh-Taylor (RT) instabilities and Kelvin-Helmholtz (KH) stripping. The ICM gas is normally composed of a live gas component that can form a shock front when a galaxy reaches supersonic velocities. Typically these studies concentrate on the highest possible resolution of the gas component of their disk galaxies, using analytical static potentials to treat the gravitational influence of the dark matter halo and stellar disk.

Our toy model does not include a live ICM gas component, so physically does not include the effects of RT instabilities or KH stripping. However, the toy model presented is fast, enabling wider parameter searches to be conducted and allowing us to include a live stellar component in our galaxy models. This is crucial to the results of this study. Furthermore, our main results arise due to the loss of the gas mass. If similar masses of gas are removed – independent of the ISM treatment – we expect similar effects as seen here. Therefore, we don’t expect our key results to change substantially if we repeated our tests with a significantly more sophisticated treatment of the ISM. Furthermore, as was demonstrated in Smith et al. (2012), despite its simplicity, the toy model can reasonably reproduce the evolution of the HI disk truncation radius in a similar manner as seen in much more complex ram pressure simulations.

3 RESULTS

3.1 Effects of ram pressure enhanced in absence of dark matter halo

TDGs may be very sensitive to ram pressure, as they are not expected to have a protective dark matter halo. To test this, we compare two dwarf galaxy models - one with a dark matter halo (we shall refer to this as the dIrr model), and an identical model but without a dark matter halo (referred to as the TDG model). The disks of both models have the properties of Model M8gf70R2, which are typical of TDGs.

We test the response of both models to three wind tunnel tests with wind speed $v_{\text{wind}}=200, 400, \text{ and } 600 \text{ km s}^{-1}$. After 2.5 Gyr of the wind tunnel test, we show the distributions of star (black points) and gas (green points) particles in Fig. 1. Disks are viewed edge-on in a 150 kpc box, although a close-up view of the stars alone is provided in the accompanying 20×13 kpc inset panels. The ram pressure wind flows upwards in each panel (in the positive z-direction).

We first consider the effects on the TDG model (upper row). Stripped gas is carried away in the direction of the ram pressure wind. For ram pressure winds with $v_{\text{wind}}=200$ or 400 km s^{-1} , the gas is not completely removed. Therefore, a truncated gas disk continues to provide a cross-section to the ram pressure wind, and so feels a drag force. The gas disk is accelerated by this force in the z-direction. As it is gravitationally bound to the stellar disk, the stellar disk also feels the drag force, and is similarly accelerated. However, this dragging mechanism can only operate efficiently on the stellar disk while gas remains in the disk. So, in the $v_{\text{wind}}=600 \text{ km s}^{-1}$ case, which quickly loses all its gas, there is little dragging.

As gas is stripped, the loss of the gas mass causes stars to be unbound. In fact, where the gas is stripped, reflects where the stars are lost. For example, if only the outer disk gas is stripped (e.g., $v_{\text{wind}}=200 \text{ km s}^{-1}$), only the outer disk stars are unbound, truncating the stellar disk in a similar way to that of the gas disk. However, if all the gas is stripped (e.g. $v_{\text{wind}}=600 \text{ km s}^{-1}$), then all the stars are unbound – *the TDG is completely destroyed*.

The final location of the stripped stars is dependent upon whether models are ram pressure stripped of all their gas, or only partially stripped. Those models that are only partially stripped (e.g., $v_{\text{wind}}=200$ and 400 km s^{-1}), suffer simultaneous unbinding of their stars and acceleration of their disk in the direction of flow of the ram pressure wind. The net result of star losses and disk acceleration is that unbound stars tend to lie in streams. Furthermore the stellar streams point in opposite directions to the gas streams in our wind tunnel tests. This is somewhat at odds with the behaviour of tidally stripped streams of stars which are more closely aligned with the gas streams (Connors et al. 2006). However, the extreme linear shape of the gas and star streams we see is almost certainly an artifact of our use of wind tunnel tests, where no external potential affects their dynamics – unlike in real TDGs.

However, models that lose all their gas very quickly (e.g., $v_{\text{wind}}=600 \text{ km s}^{-1}$) suffer little dragging, and so unbound stars expand away from the TDGs centre in a roughly isotropic manner, creating an expanding envelope.

Now we compare the effects of the wind tunnel tests on the TDG model to the dIrr model that has a dark matter

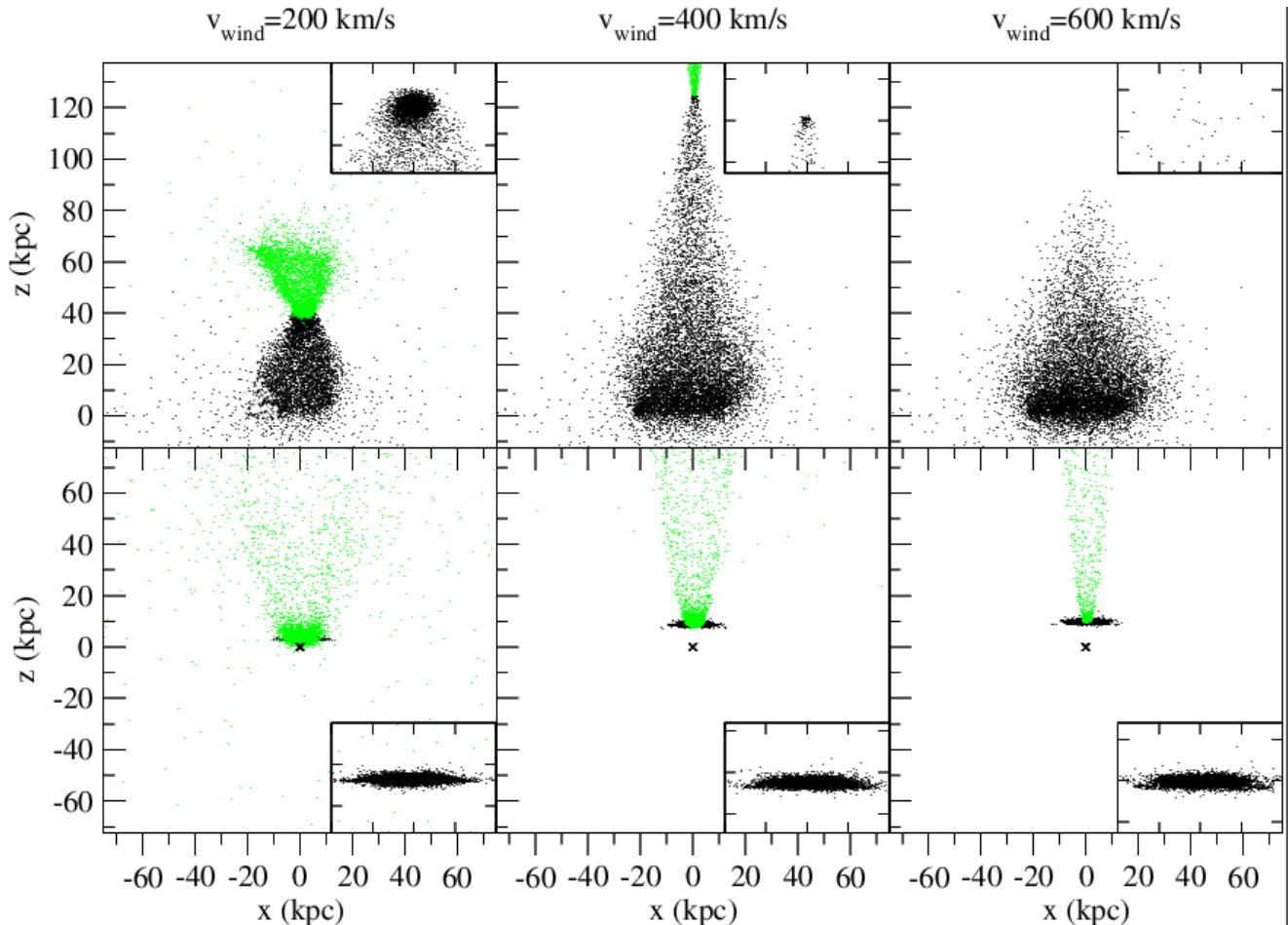


Figure 1. The impact of ram pressure stripping on the stars (black points) and gas (green points) of a model dwarf galaxy (M8gf70R2) in a 150 kpc sided box. In the lower panels the model has a dark matter halo (like a typical dIrr). In the upper panels there is no dark matter halo (like a TDG). Ram pressure wind speeds of $v_{\text{wind}}=200$, 400, and 600 km s^{-1} (left, middle, and right columns) are presented. A ‘close-up’ image of the stars only is shown in a corner sub panel spanning 20.0 by 13.3 kpc. Without a dark matter halo (upper panels), the effects of ram pressure are dramatic. Ram pressure stripping can cause significant stellar losses. The galaxy’s stellar disk is also accelerated by ram pressure drag acting on the remaining gas disk, causing stars to lie in a stream pointing away from the gas stream. If the gas is rapidly stripped altogether (e.g., $v_{\text{wind}}=600 \text{ km s}^{-1}$), there is little dragging, but the TDG is completely unbound. With a dark matter halo (lower panel), the dwarf galaxy is much more stable to ram pressure stripping. There are no stellar losses. Ram pressure results in much weaker acceleration of the stellar disk. The stellar disk merely thickens by a factor ~ 2 in response to the loss of the gas mass.

halo (in the lower panels of Fig. 1). The dIrr model also suffers ram pressure drag, however the resulting acceleration is much less significant. We indicate the initial position of the disk with a cross symbol. The gas disk continues to feel a drag force, like in the TDG model, but now the drag force must be shared between the the stellar disk *and* the dark matter surrounding the disk. As the additional mass of the dark matter must be towed, the resulting acceleration is much weaker.

There is no unbinding of stars in the dIrr model, and hence no stellar streams. The loss of the gas mass causes a much less dramatic effect on the stellar dynamics. This is because the dark matter potential plays a strong role in influencing the stellar dynamics in the dIrr model. The response of the stars is limited to a thickening of the stellar disk by a factor ~ 2 , due to the presence of the dark matter. We note that a thorough investigation of the effects of ram

pressure stripping on dark matter dominated dwarfs can be found in Smith et al. (2012).

In summary, due to an absence of dark matter in our model TDG, the effects of ram pressure are very dramatic. Although ram pressure only directly impacts upon the gas component of the TDG, the loss of the gas can have a very substantial effect on its stellar disk. Stars are unbound, the disk is accelerated, and the entire TDG is destroyed when the gas is fully stripped.

3.2 Tidal Dwarf galaxy disruption through ram pressure

We have so far only considered a single TDG model – Model M8gf70R2. In the following section we better quantify the loss of gas and stars for TDGs with a variety of properties, each experiencing different strengths of ram pressure. A full

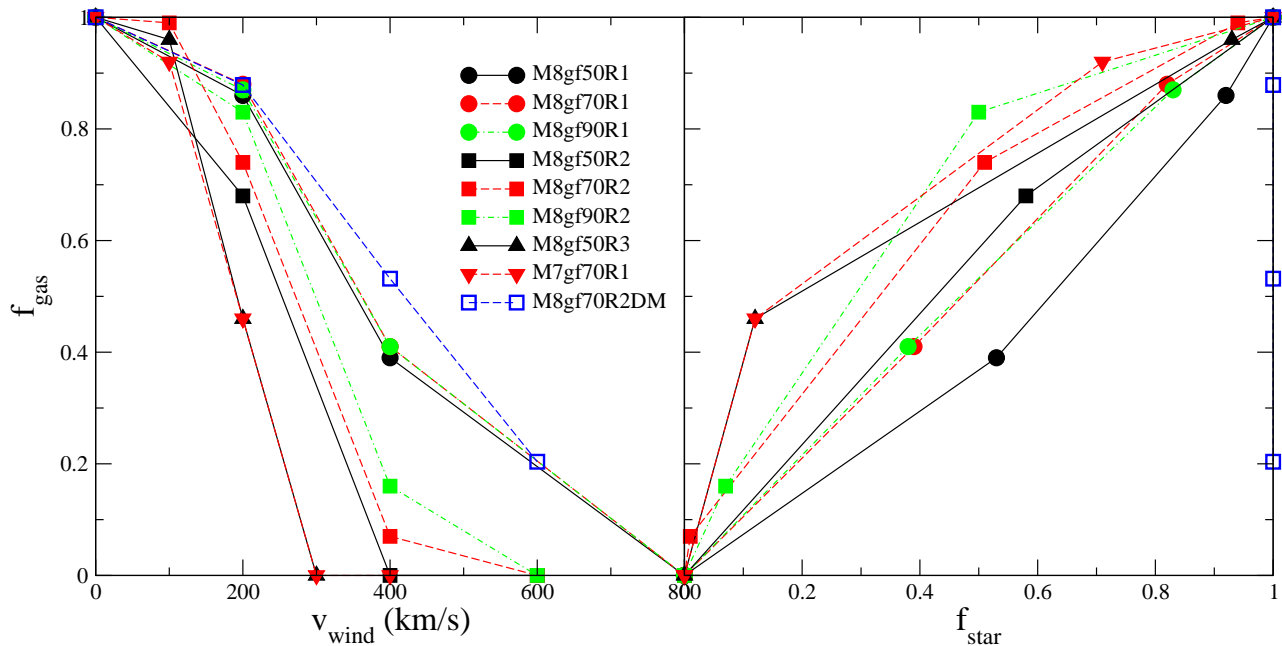


Figure 2. (left) Fraction of gas remaining bound f_{gas} after wind tunnel tests with different wind speeds v_{wind} . Symbol and line style indicates model galaxy. Models with lower central surface density (i.e large effective radius or low total mass) are stripped for lower wind speeds. (right) Fraction of gas f_{gas} that remains bound compared to the fraction of stars that remain bound f_{star} . In general, the amount of gas that is stripped is roughly equal to the amount of stars that become unbound for our model TDGs. As the stars and gas are distributed in the same manner, this reflects the fact that the stars are unbound at the same radii where the gas is stripped. TDG Model M8gf70R2 (red squares) is the same as dIrr Model M8gf70R2DM (blue empty squares) except the latter has a dark matter halo. No stars are lost in the model with a dark matter halo. Also gas losses are reduced in the model with a halo, in part from the increased gravitational restoring force of the galaxy.

list of the model TDGs we consider, and the speed of the wind in each wind tunnel test, is given in Table 1.

We record the final bound fractions of stars f_{star} , and gas f_{gas} , for each model, after each wind tunnel test at $t=2.5$ Gyr. To measure if a star or gas particle is bound to the TDG, we use the ‘snowballing’ method described in Smith et al. (2013). The results are shown in Fig. 2. The left panel shows the dependency of f_{gas} on the ram pressure wind speed, for each model TDG (see the key). As expected, stronger wind speeds causes more gas to be stripped. Those models with lower central surface densities are most sensitive to gas stripping by ram pressure. These include models with larger effective radii (e.g M8gf50R3), or lower mass (e.g. M7gf70R1), which lose about half their gas at $v_{\text{wind}}=200$ km s $^{-1}$, and are entirely stripped of their gas at $v_{\text{wind}}=300$ km s $^{-1}$. Ram pressure winds with $v_{\text{wind}}\sim 200$ km s $^{-1}$ are expected for some dwarf galaxies bound to the MW, while winds on the order of $v_{\text{wind}}\geq 300$ km s $^{-1}$ are expected in group environments. Higher surface density models, such as those with an effective radius of 1 kpc (M8gf50R1-M8gf90R1), lose roughly half their gas at $v_{\text{wind}}=400$ km s $^{-1}$ (galaxy group velocities), and are not completely stripped until $v_{\text{wind}}=800$ km s $^{-1}$ (galaxy cluster velocities).

The right panel of Fig. 2 allows us to compare f_{gas} to f_{star} for all simulations in our parameter study. In general, we see that almost all models suffer roughly equal fractions of stars and gas being stripped. For example, if a model has half its gas stripped, then roughly half its stars are unbound in the process. This corroborates the point made ear-

lier that stars are unbound where the gas is lost, as the gas is initially distributed in a disk with the same scalelength as the stars. Therefore, if the gas was more extended than the stars, then we might expect preferential loss of gas over stars (Connors et al. 2006).

In the previous section, we compared the difference in the appearance of Model M8gf70R2 after undergoing ram pressure with, and without, a dark matter halo surrounding the disk (see Fig. 1). Now we include the model with a halo in Fig. 2 so we can investigate how baryonic mass loss depends on the presence of a halo. The dark matter dominated model is referred to as Model M8gf70R2DM (open blue squares), whereas the dark matter free TDG model is Model M8gf70R2 (filled red squares). The model with a dark matter halo suffers no stellar losses at all, even when a large fraction of the gas is stripped. We also see that less gas is stripped in the model with a dark matter halo. This occurs partly due to the enhanced gravitational restoring force from the dark matter halo (Abadi et al. 1999). Also, when there is no dark matter halo surrounding the disk, the stars near the truncation radius maybe highly perturbed by the gas removal. This may also play a role in enhancing gas losses in TDGs.

3.3 Stellar disk acceleration by ram pressure drag, and enhanced stellar losses

We now investigate the degree of acceleration that the stellar disk of a TDG undergoing ram pressure might experience. Therefore, we record the total change in velocity that occurs

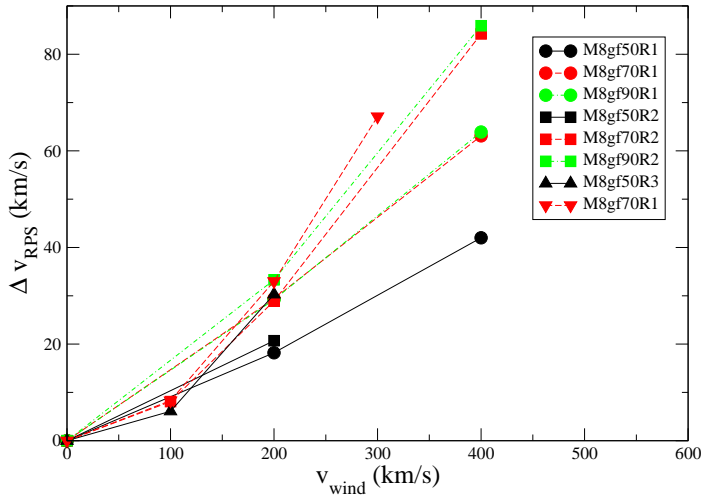


Figure 3. The gas disk experiences a drag force which is shared with the stellar disk through their gravitational interaction. We measure the change in velocity of the bound stellar disk of the model as a result of ram pressure drag ΔV_{RPS} and plot it versus the wind speed v_{wind} in the wind tunnel test. Changes in velocity by 20-80 km s⁻¹ are typical. Most lines end abruptly at higher ram pressure winds when models are entirely stripped of their gas and their stellar disk is destroyed, so as the change in velocity of the bound stellar disk can no longer be measured.

to the stellar disk as a result of ram pressure ΔV_{RPS} , after 2.5 Gyr of each wind tunnel test. We measure ΔV_{RPS} for all the tests in our parameter study, to try to understand any dependency on TDG properties.

The results are shown in Fig. 3 for each model TDG (see symbols and line styles in the accompanying key). Most models show a total change in velocity due to ram pressure drag of 20-80 km s⁻¹. We measure the velocity of the bound stars, therefore most models have lines that abruptly end at an upper v_{wind} when their gas is stripped, and the stars become unbound. This complicates the clear detection of a simple relationship between amount of acceleration and TDG properties, as it is convolved with a dependency on survival to ram pressure. As a result, we do not see a trivial dependency on model properties. However, we emphasise that a change in velocity of ~ 80 km s⁻¹ may be significant for altering orbital properties of TDGs, in particular where the velocity change is a significant fraction of the galaxy’s orbital velocity. As we will now demonstrate, the change in velocity of the TDG disk also has consequences for the number of stars that are unbound.

To demonstrate that stars are lost due to acceleration of the TDG, we consider a low gas fraction model (30% gas, 70% stars): M8gf30R2. We submit this model to four ram pressure wind tunnel tests for 2.5 Gyr ($v_{\text{wind}}=200, 300, 400$ and 600 km s⁻¹) and measure the final bound fraction of stars f_{star} , and gas f_{gas} . We also test the resulting f_{star} , allowing for instantaneous removal of the gas. This ‘instant gas mass loss’ case allows us to see the effects of the removal of the gas mass without the additional effects, such as ram pressure dragging, that we see in the wind-tunnel test.

This latter case is shown in Fig. 4. The upper panel shows the final f_{star} (black line) and f_{gas} (red line) of the TDG model in the wind tunnel tests with wind speed v_{wind}

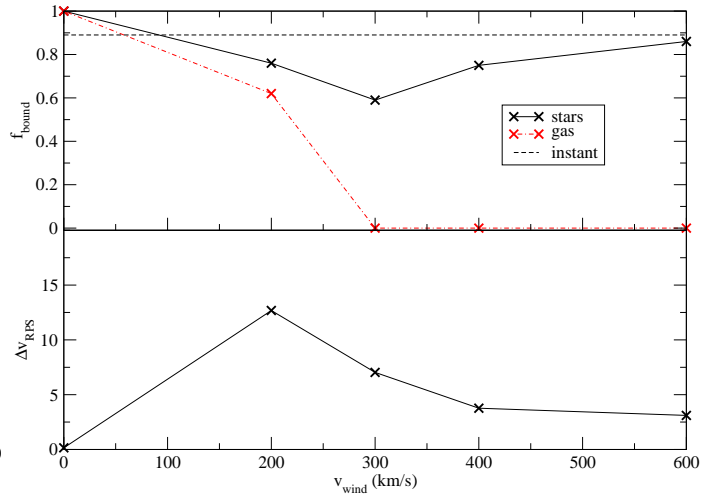


Figure 4. For model M8gf30R2; (upper) fraction of stars f_{star} (black solid line), and fraction of gas f_{gas} (red dash-dot curve) as a function of wind speed in each wind tunnel test. The dashed horizontal line indicates f_{star} after instantaneous removal of the gas. (lower panel) Change in velocity of the stellar disk of the model as a result of ram pressure drag ΔV_{RPS} . Stars are unbound due to the loss of the gas potential. However, acceleration of the stellar disk by ram pressure drag, further enhances stellar losses. For example (see upper panel) ram pressure stripped models experiences greater stellar losses than occur when the gas is instantaneously removed. Also, if the gas is totally stripped (see lower panel), models that have experienced the greatest acceleration due to ram pressure suffer larger stellar losses.

(shown on the x-axis). The dashed horizontal line indicates the final f_{gas} of the model after instantaneous gas loss. In all the wind tunnel tests, the model loses *more* stars than in the instantaneous gas loss case.

The latter is somewhat surprising, as the instant gas loss case sets an upper limit on the number of stars that are unbound by the loss of the gas potential alone. Instant gas loss gives no time for the stars to respond to the changing potential, whereas the loss of the gas is not so quick in our wind tunnel tests, so the stars have more time to respond to the changing potential. In fact, even more surprising is the wind tunnel test with $v_{\text{wind}}=200$ km s⁻¹ – *the model loses less than half its gas, and still more stars are unbound than when all the gas is lost instantaneously.*

These results highlight the presence of an additional mechanism that causes stars to be unbound, and in greater quantities than can occur from the loss of the gas potential alone. We find that the additional mechanism is due to acceleration of the TDG disk by ram pressure drag. This can be understood if we consider the accelerating frame of reference of a TDG undergoing ram pressure drag. Stars are liberated from the disk by the loss of gas mass. If the TDG were not accelerating, some stars would remain marginally bound and eventually infall back towards the disk. However, due to the acceleration of the TDG since the stars were emitted, these stars are left behind. This is apparent when we plot the change in velocity of the stellar disk as a result of ram pressure ΔV_{RPS} in the lower panel of Fig. 4. When the gas is fully stripped ($v_{\text{wind}} \geq 200$ km s⁻¹), models that accelerate the most (i.e with the highest values of ΔV_{RPS}) lose more stars. We note that as v_{wind} increases from 300 km s⁻¹

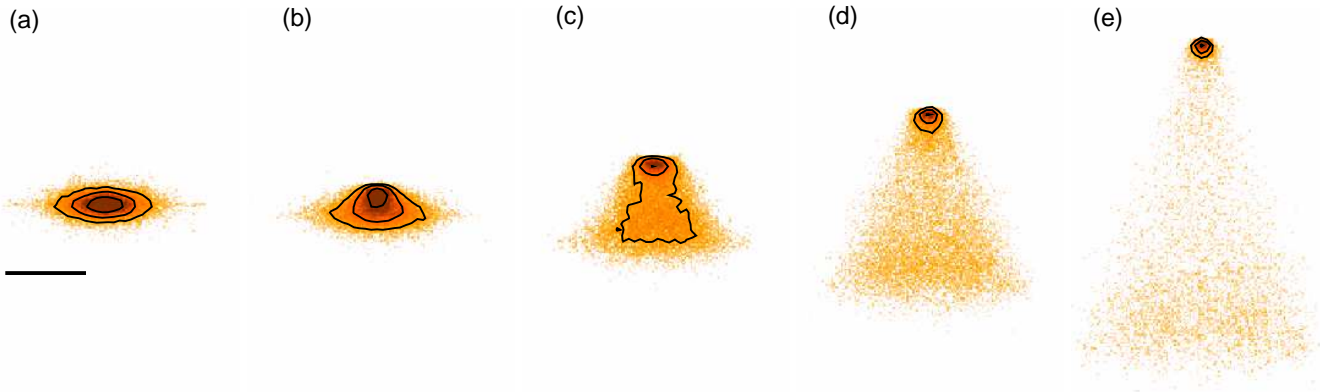


Figure 5. Snapshots of surface brightness time-evolution of Model M8gf50R3 at time = (a) 0.000 Gyr, (b) 0.625 Gyr, (c) 1.250 Gyr, (d) 1.875 Gyr, (e) 2.500 Gyr. Length of solid bold line on left of figure indicates scale of 10 kpc. Intensity of colour indicates surface brightness, with contours shown at 29, 30, 31 $\text{mag}_V \text{arcsec}^{-2}$. For simplicity we assume a stellar mass-to-light ratio of 1 in all surface brightness calculations (although this may be very incorrect for a young stellar population).

to 600 km s^{-1} , the fraction of bound stars approaches the instantaneous gas expulsion value. This is to be expected as an increasing v_{wind} leads to an increasingly rapid total removal of the gas.

We have demonstrated the effects of disk acceleration on f_{star} with a (somewhat unrealistic) low gas fraction model, simply because instantaneous gas loss results in the destruction of all the other models, therefore hiding the effects of the disk acceleration. However, loss of stars due to gas mass loss, combined with acceleration due to ram pressure drag, undoubtedly occurs in all our ram pressure stripped models.

3.4 Formation of stellar streams by ram pressure

Stellar losses, combined with acceleration by ram pressure drag, causes stars to lie in a low surface brightness stream behind the accelerated TDG. In Fig. 5 we show the stream produced by Model M8gf50R3. Each image is a snapshot at 0.625 Gyr intervals, ranging from $t=0$ Gyr to $t=2.5$ Gyr. The bold line indicates a 10 kpc scale. The intensity is proportional to the logarithm of the mass surface density. We include a surface brightness contour at 29, 30, 31 $\text{mag}_V \text{arcsec}^{-2}$, assuming a V-band stellar mass-to-light ratio (M/L_V) of 1. We note that this choice of stellar mass-to-light ratio may be incorrect, as unbound stars may consist of a complex mix of young and old stellar populations. However, as we do not include star formation in our models, we cannot provide detailed predictions of the stellar populations in the streams, and for simplicity choose a single fixed value of unity.³

By $t=1.25$ Gyr, an ~ 15 kpc stream has been drawn out. By 2.5 Gyr the stream is ~ 40 kpc long. With increasing length, the stream decreases in surface brightness. What is apparent is that the long streams are of very low surface brightness. Even the relatively bright stream at $t=1.25$ Gyr (panel c), is only seen at $>31 \text{ mag}_V \text{arcsec}^{-2}$ (assuming $M/L_V=1$). Such low surface brightness streams may only be

detected surrounding Local Group galaxies, and even then only from star counts. For this stream to be visible at the level of $29 \text{ mag}_V \text{arcsec}^{-2}$, the stellar population must be ~ 6 times brighter than we have assumed. However the situation at $t=0.625$ Gyr (panel b) may be more easily detected, when the core of the galaxy is several kiloparsecs off-centre within a surrounding low surface brightness envelope.

3.5 Effects on mass Sersic profiles

We now examine the effects of stellar losses on the stellar surface density profiles. We restrict ourselves to studying the evolution of the *mass* surface density, and not the luminosity. In Fig. 6, we show the stellar particle distribution of Model M8gf70R2 before ram pressure (first row), and after undergoing three wind tunnel tests: $v_{\text{wind}}=200, 400, 600 \text{ km s}^{-1}$ (second, third, and fourth row respectively). The left and right column shows the TDG viewed face-on and edge-on respectively.

We produce fits images of the stellar mass distribution using the IRAF *rtextimage* task. Our fits images cover a 20 by 20 kpc region for the pre-ram pressure model, and $v_{\text{wind}}=200$ and 400 km s^{-1} models. We use a 40 by 40 kpc region fits image for the $v_{\text{wind}}=600 \text{ km s}^{-1}$ model. We measure the surface density profile of the stars using the IRAF *ellipse* task, without restricting the radial range to be fitted. The resulting mass surface density profile of the stars is then fitted over the complete radial range using a generalised Sersic profile (Caon et al. 1993):

$$\Sigma(R) = \Sigma_{\text{eff}} \exp \left(-b_n \left[\left(\frac{R}{R_{\text{eff}}} \right)^{1/n} - 1 \right] \right) \quad (9)$$

where $b_n = 1.9992n - 0.3271$, n is the Sersic index, R_{eff} is the effective radius, and Σ_{eff} is the surface density at R_{eff} . The best-fit values are shown above each panel in Fig. 6.

Prior to ram pressure (upper row), the stellar distribution is close to exponential ($n \sim 1$), and the effective radius is approximately 2 kpc. However, after the 200 km s^{-1} wind tunnel test (second row), the outer disk gas has been stripped, resulting in unbinding of the outer disk stars. This truncates the stellar disk, in the same way as the gas disk

³ If we assume a younger, brighter population with $M/L_V=0.25$, the value associated with each surface brightness contour decreases by one magnitude.

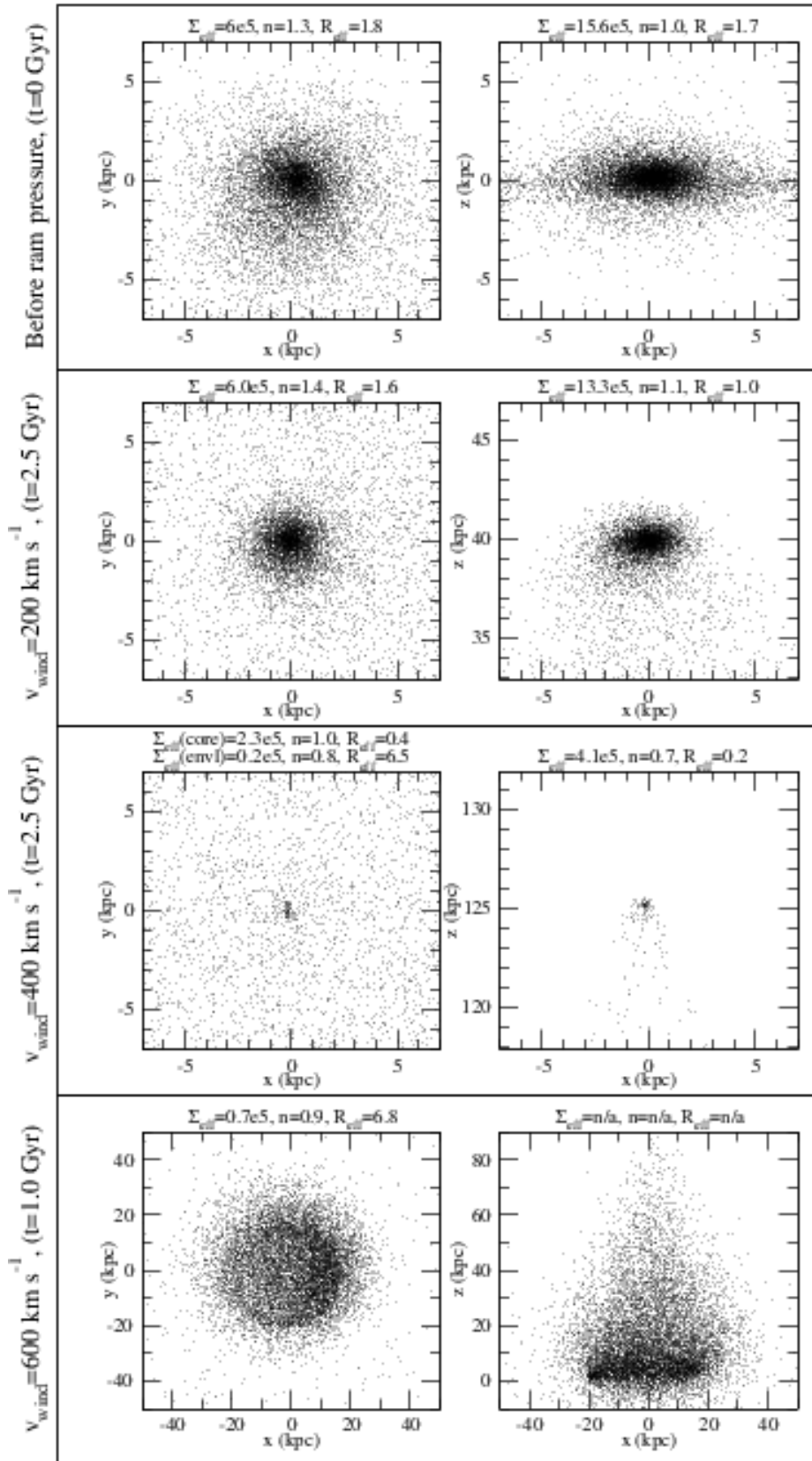


Figure 6. Face-on (left column) and edge-on (right column) snapshots of the star particle distribution of Model M8gf70R2 following wind tunnel tests with wind speed $v_{\text{wind}}=200, 400, 600 \text{ km s}^{-1}$ (second, third, and fourth row respectively). Above each panel, the parameters of the Sersic fit to the mass distribution are shown; surface density within the effective radius (Σ_{eff}), the Sersic index (n), and the effective radius (R_{eff}). In general, the Sersic index remains near $n \sim 1$. However R_{eff} can be reduced by preferential loss of outer disk stars in TDGs that are not completely stripped of their gas. Or if the gas is rapidly stripped, the expanding unbound stars can have very large R_{eff} , but coupled with low Σ_{eff} .

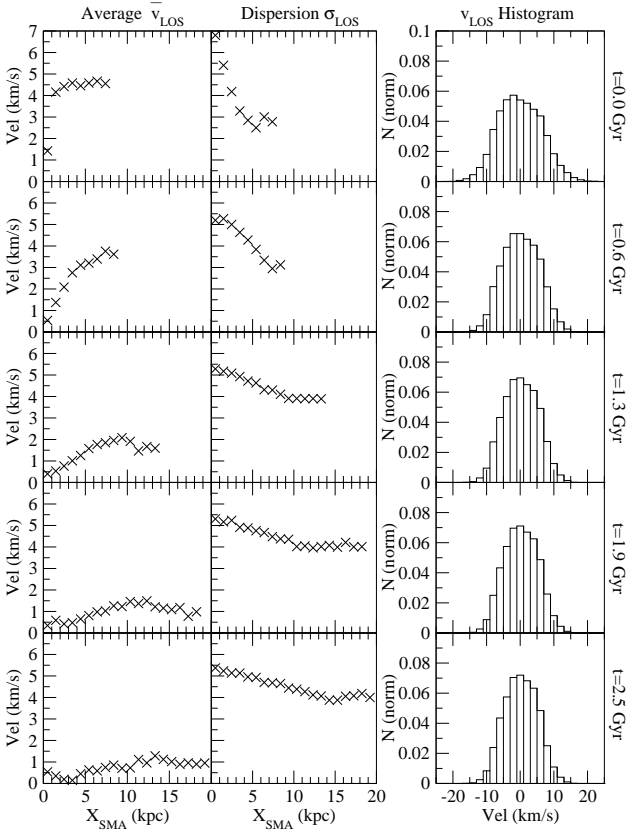


Figure 7. Plots of the line-of-sight velocities of Model M8gf70R2, viewed along the y-axis so as the disk is seen edge-on. In column 1 and 2, velocities are binned along the semi-major axis of M8gf70R2. Column 1 is the average velocity in each bin (so indicates rotation). Column 2 is the velocity dispersion in each bin. Column 3 is a histogram of the line-of-sight velocities of all the star particles. Each row is from a specific time (snapshot time is shown along the right-hand edge of Column 3). The model undergoes a wind tunnel test with $v_{\text{wind}}=600 \text{ km s}^{-1}$. All the gas is stripped, causing the stars to be totally unbound, by $t=0.6 \text{ Gyr}$. The peak of the rotation curve decreases, and the velocity dispersion profile flattens as the unbound stars expand. However, if viewed at only one instant, there is no clear indication that the stars are actually unbound and expanding, in either the radial plots or the velocity histograms.

has been truncated, at a radius $R \sim 3 \text{ kpc}$. The stellar disk inside the truncation radius remains roughly exponential. However, the loss of the outer disk stars causes the effective radius to be reduced.

A similar but more extreme example is seen in the 400 km s^{-1} wind tunnel test (third row). Now the gas and stellar disks are heavily truncated at $R < 0.5 \text{ kpc}$. Once again, the remaining stellar disk is roughly exponential, but now the effective radius has been significantly reduced. Viewed face-on (left panel), the presence of large numbers of stripped stars down our line-of-sight causes a low surface density envelope to appear around the heavily truncated stellar disk. There is no attempt to make a cut in the z-direction, therefore the line-of-sight contains all the star particles possible. We fit the surface profile of the truncated stellar disk (or ‘core’) separately from the surrounding envelope. This is accomplished by only fitting data points at

$R > 1.0 \text{ kpc}$ for the envelope, and points at $R < 0.5 \text{ kpc}$ for the core. The envelope also has a roughly exponential profile ($n \sim 1$), although the effective radius is very large ($\sim 6 \text{ kpc}$).

A rather different surface density profile occurs if stripping of all the gas occurs rapidly, such that there is little dragging. The loss of all the gas completely unbinds the stellar disk, and the lack of dragging means unbound stars do not form a stream. Instead, they expand outwards from the centre of the TDG in an envelope. This is seen in the 600 km s^{-1} wind tunnel test (bottom row). As all the stars are unbound, we find the mass profile evolves rapidly with time. It becomes difficult to measure the parameters of the generalised Sersic profile beyond 1 Gyr. However, over $\sim 1 \text{ Gyr}$ of evolution, the profile remains roughly exponential ($n \sim 1$), becomes very low surface brightness, and increases its effective radius from $\sim 2 \text{ kpc}$ to $\sim 6 \text{ kpc}$.

In summary, the surface density profiles of our ram pressure stripped models are all roughly exponential. However, if the TDG disk is not completely stripped of gas, stars in the outer disk are unbound where the gas has been lost. This causes the remaining stellar disk to be truncated, resulting in a reduced effective radius. On the contrary, if the gas is completely stripped from the TDG model, the stars are completely unbound, causing the effective radius to grow with time, while decreasing the surface brightness.

3.6 Effects on stellar dynamics and implications for dynamical mass measurements

We now examine the effects of ram pressure stripping on the dynamics of stars in our models. As stars are unbound when the gas is stripped, the dynamics of the unbound stars down our line-of-sight may potentially affect measurements of a TDG’s dynamical mass from its stellar dynamics if dynamical equilibrium is assumed.

First we examine the stellar dynamics of the Model M8gf70R2. We study the time evolution of the stellar dynamics as viewed down a line-of-sight. We choose a sightline that is edge-on to the disk, as this best enables us to measure signatures of rotation. We arbitrarily choose the y-axis as our line-of-sight, although our results show negligible change if we had instead chosen the x-axis. We bin the line-of-sight velocities of all stars along the semi-major axis of the disk, and calculate the average and standard deviation of the stellar velocities within that bin. Any trace of rotation should be visible in the profile of the average velocity.

The results for the wind tunnel test with $v_{\text{wind}}=600 \text{ km s}^{-1}$ are shown in Fig. 7. Recall from the previous section that this model is quickly stripped of all its gas, causing the stellar disk to become totally unbound. The unbound stars form an expanding envelope. Column 1 shows the average, and the Column 2 shows the standard deviation, of the velocities in a bin, plotted against the distance along the semi-major axis X_{SMA} . We include all star particles that fall in a bin of X_{SMA} in the average and standard deviation calculation, without considering their z-position. Although we find negligible change in our results if we include only stars with $|z| < 10 \text{ kpc}$ from the TDG centre. However, we neglect data points with less than 50 stars in a bin to avoid low-N noise.

The bins of average velocity (Column 1) show that a signature of rotation remains within the expanding envelope,

although the peak value decreases. This shows the decreasing speed of rotation as the disk expands, as required for angular momentum conservation. Likewise, the velocity dispersion profile (Column 2) becomes steadily flattened as the envelope expands.

Close to the core of the model ($X_{\text{SMA}} < 2$ kpc), one is clearly dominated by dispersion even before ram pressure, and this remains the case afterwards. However, prior to ram pressure, in the outer disk ($X_{\text{SMA}} > 5$ kpc), rotation dominates dispersion. After ram pressure stripping, the dispersion in the outer disk tends to increase, while rotation tends to decrease. The net effect is a decrease in rotation-to-dispersion ratios, especially in the outer disk.

Interestingly, if we consider only one snapshot in time, there is no clear signature in either the average or standard deviation of the binned velocities indicating that the model is unbound and expanding. To look for another signature of the expansion, we plot histograms of the line-of-sight velocities of all the stars in a snapshot. These are shown in Column 3 of Fig. 7. If all the stars were expanding towards and away from us down our line-of-sight with a roughly equal expansion velocity, we would see a double peak in the velocity histogram. In fact the stars expand with a smooth spread in velocities, so as there is no double peak of velocities. *Therefore a TDG model that is completely and rapidly stripped of its gas shows very little indication that it has been entirely unbound if viewed at one instant.* Recalling from the previous section, such a TDG remains near exponential, but steadily grows in size, decreasing its surface brightness while increasing its effective radius, and yet shows little indication of the fact it is unbound in its line-of-sight dynamics.

Therefore, in some circumstances, ram pressure disrupted TDGs might be confused with other types of dwarf galaxies. With time the effective radius of our disrupted TDG model M8gf70R2 grows very large, and this might naively be expected to differentiate it from other dwarfs. However our effective radii are measured in the idealised situation when there is no background light, whereas in observations of real dwarfs the low surface brightness outer edges of the surface brightness profile may be lost in the background. If not correctly accounted for, this could result in measurements of the effective radius that are smaller than we measure in the models. Furthermore, our models do not consider the surrounding tidal field, that can preferentially truncate and strip the stars with the largest radii, physically reducing the effective radius. Also, we see no obvious reason why TDGs that start off much smaller, and are then disrupted by ram pressure, might not expand to have properties that overlap with those of other dwarf galaxies. The lack of dark matter, as seen in the stellar dynamics of a TDG, might also be expected to differentiate a TDG from another dwarf galaxy. However, as we will now demonstrate, the effect of ram pressure on the stellar dynamics of a TDG can mimic the presence of substantial quantities of dark matter.

In order to measure dynamical masses of galaxies, using their observed stellar dynamics, the stars are typically assumed to be in dynamical equilibrium with the galaxy's potential. However, our models show that ram pressure stripped TDGs have many stars unbound. The presence of unbound stars down our line-of-sight would violate the assumption of dynamical equilibrium, and may potentially re-

sult in dynamical masses that appear greater than the true mass. We attempt to quantify this effect now.

Following a similar approach as described in Evans et al. (2003) (and applied in Beasley et al. 2006; Beasley et al. 2009), we separate the total dynamical mass of a galaxy model M_{dyn} into a dynamical mass supported by pressure M_{press} , and a dynamical mass supported by rotation M_{rot} such that $M_{\text{dyn}} = M_{\text{press}} + M_{\text{rot}}$.

We calculate M_{dyn} at the half-mass radius $r_{1/2}$. For the pressure supported dynamical mass, we use $M_{\text{press}}(r < r_{1/2} = 3 G^{-1} < \sigma_{\text{LOS}}^2 > r_{1/2}$ (Wolf et al. 2010) where $< \sigma_{\text{LOS}}^2 >$ is the square of the line-of-sight velocity dispersion measured within r_{eff} . This approach minimises the potential influence of velocity anisotropy on M_{press} . We calculate the rotation-supported dynamical mass at $r_{1/2}$ using $M_{\text{rot}} = r_{1/2} G^{-1} v_{\text{rot}}^2$ where v_{rot} is the value of the average velocity, down our line-of-sight, measured at $r_{1/2}$. Having calculated the total dynamical mass, we then normalise it by the true mass M_{real} also measured within $r_{1/2}$. Specifically M_{real} is the total mass, bound or unbound, found within a sphere of radius $r_{1/2}$. The ratio $M_{\text{dyn}}/M_{\text{real}}$ is a measure of how well the dynamical mass agrees with the true mass (e.g., if $M_{\text{dyn}}/M_{\text{real}} \equiv 1$, the dynamical mass is in perfect agreement with the true mass).

As in the previous section, we consider Model M8gf70R2, evolved in isolation, and undergoing the same three wind tunnel tests: $v_{\text{wind}}=200, 400, \text{ and } 600 \text{ km s}^{-1}$. We consider an edge-on view to the disk (see right column of Fig. 6 for the final distribution of stars in each wind tunnel test along this line-of-sight). We follow the time evolution of the ratio $M_{\text{dyn}}/M_{\text{real}}$.

We first consider the model evolved for 2.5 Gyr in isolation. In isolation, we measure $M_{\text{dyn}}/M_{\text{real}}=1.08, 0.90, 0.97, 0.93, 0.98, \text{ and } 1.02$, when measured at $t = 0, 0.5, 1.0, 1.5, 2.0$ and 2.5 Gyr, respectively. Thus, our technique for measuring the dynamical mass appears reliable to within $\sim 10\%$ of the true mass.

Next, we consider the $v_{\text{wind}}=600 \text{ km s}^{-1}$ wind tunnel test, where the model was quickly stripped of all its gas, resulting in an expanding envelope of unbound stars. We measure $M_{\text{dyn}}/M_{\text{real}}=1.1, 2.0, 6.1, 7.3, 8.0, 10.7, \text{ and } 12.7$, when measured at $t = 0.00, 0.25, 0.50, 0.63, 0.75, 1.00, \text{ and } 1.25$ Gyr, respectively. As expected, by assuming dynamical equilibrium, our technique finds dynamical masses that are heavily in excess of the real mass. The excess increases as the envelope expands.

Finally, we consider the wind tunnel tests with $v_{\text{wind}}=200$ and 400 km s^{-1} . Recalling from the previous section, the model stellar disk suffers a mild disk truncation in the outer disk for $v_{\text{wind}}=200 \text{ km s}^{-1}$ (see right panel of second row in Fig. 6). The disk truncation is much more severe for $v_{\text{wind}}=400 \text{ km s}^{-1}$, and only a small stellar disk remains (see right panel of third row in Fig. 6). However, in both these cases, where a bound stellar disk remains, disk dragging has caused the unbound stars to be drawn into a stellar stream. Therefore there are fewer unbound stars seen down our line-of-sight, and their effect on mass estimates is greatly reduced. For $v_{\text{wind}}=200 \text{ km s}^{-1}$, we measure $M_{\text{dyn}}/M_{\text{real}}=1.02, 1.09, 1.10, 1.13, 1.22, \text{ and } 1.29$ at $t=0.0, 0.5, 1.0, 1.5, 2.0, \text{ and } 2.5$ Gyr. For the more heavily truncated stellar disk with $v_{\text{wind}}=400 \text{ km s}^{-1}$, we measure

$M_{\text{dyn}}/M_{\text{real}}=1.03, 1.69, 1.40, 1.35, 1.49,$ and 2.20 at $t=0.0, 0.5, 1.0, 1.5, 2.0,$ and 2.5 Gyr.

In summary, the effect of ram pressure stripping on TDG stellar dynamics causes stars to be unbound, which in turn increase the apparent (empirically-derived) dynamical mass. When our TDG model is completely stripped of gas, its stars are completely unbound, and form an expanding and rotating envelope. In this situation, measurements of the dynamical mass may be substantially greater than the true mass by factors of ~ 10 . However, when the gas is not completely stripped and a bound stellar disk remains, the effect of unbound stars is much weaker. In this case, our dynamical masses are typically no more than double the true mass.

4 DISCUSSION

In this study, we have demonstrated that a lack of dark matter in tidal dwarf galaxies, coupled with high gas fractions, makes them very sensitive to ram pressure stripping. At radii where the gas is stripped from the disk, the stars are unbound. Stellar streams are often attributed to the actions of tides. Here we show that even ram pressure may play a role in shaping them. In fact, if the gas is completely stripped, we find that the TDG models are destroyed altogether. We find it difficult to see how TDGs can survive the loss of their disk gas unless the relative densities of gas to stars within the disk is much lower than we have assumed.

Based on these results, TDGs that survive by maintaining their gas disks against ram pressure can perhaps be expected to have undergone particular evolutionary scenarios. They may have formed with small, relatively high surface brightness disks or have large masses. This provides them with greater disk self-gravity such that they are better able to hold onto their gas. Alternatively, they may form at large radii from their interacting progenitor galaxies, where the hot gaseous halos are low density. Their subsequent orbits may also be constrained so as to avoid plunging orbits past the progenitor galaxies, where combined high orbital velocity and high densities of hot gas could result in strong ram pressures, and therefore destruction. Plunging orbits near to the progenitors could also result in strong tidal forces, causing tidal stripping of stars and gas – an additional mass-loss effect which we have not included in our models. Some TDGs may have only recently formed, so there has been insufficient time for the gas to be stripped, or prior to the first pericentre of their orbit past the progenitor galaxies. We note another possibility – some TDGs may actually have been stripped of their gas, and been completely unbound. Our TDG models that suffered this fate do not show clear indications of being unbound, either visually, or in their stellar dynamics, beyond a steady decrease in surface density with increasing effective radius.

In fact, we suspect that a strong dynamical response of stars to gas removal by ram pressure is not limited to the TDGs themselves. The tidal streams of stars and gas that give birth to, and feed, newly formed TDGs should be even more sensitive to ram pressure. These streams are also expected to be gas rich, and are not dominated by dark matter. Given their low surface densities, and so weak self-gravity, they should be stripped of their gas for weaker ram

pressures than the TDGs themselves. Even if ram pressure is unable to strip the gas from the TDGs, it may still play a role in altering a TDGs evolution by stripping tidal streams, therefore cutting off fresh supplies of gas and stars.

What might we expect if a tidal streams suffers ram pressure? In fact given the destructive impact on our TDG models, it is likely that the stars in an initially gas rich tidal tail would be dissipated following ram pressure stripping. In this scenario, stellar-only streams would generally only be produced by the tidal dissolution of a galaxies, as ram pressure stripping may be too destructive to the stellar component of a gas rich tidal stream.

Given that tidal streams should be even more sensitive to ram pressure than TDGs, this raises the question: why are the gas and stars so well aligned in many tidal streams? Examples include the M81 group (Yun et al. 1994), NGC4676 (Hibbard & van Gorkom 1996), NGC2992/3 (Duc et al. 2000), and NGC4038/39 (Hibbard et al. 2001). Although offsets can be found between the gas and stellar distribution in some tidal streams (e.g., Arp 299; Hibbard & Yun 1999), these can be largely explained by differences in the initial distribution of the gas compared to the stars, and the dissipational nature of the gas compared to the dissipationless nature of the stars (Mihos 2001). One possibility is that the streams can only exist where the ram pressure is weak – at large radii where the hot gas density is low, and the velocity of the streams relative to the hot gas is low. The streams of cold gas may also temporarily be able to shield themselves by being enveloped in a their own hot gas that moves with the stream. This envelope must first be stripped, before cold stream can directly feel the ram pressure. A similar process is proposed to occur in disk galaxies within the galaxy cluster environment (Bekki 2009). Alternatively, the hot gas halos may be flowing themselves, and gas streams may only form where they do not oppose the flow of the hot gas. An understanding of the dynamics of the hot gaseous halos of interacting galaxies may be vital for understanding the evolution of tidal streams and TDGs.

If we assume that TDGs and tidal streams are very sensitive to ram pressure, then we can use them as probes of their local environment. If, in general, they show no indication of ram pressure, perhaps the hot gaseous halos surrounding the TDGs are much lower density than we have been assuming. This would be very unexpected. For example, we choose the density of hot gas in our simulation to be typical of the measured density of the MW gaseous halo (Bregman & Lloyd-Davies 2007; Lehner et al. 2011; Gupta et al. 2012). In fact, we might expect significantly higher hot gas densities in strongly interacting galaxies where compressive tidal forces and supernovae feedback may convert large quantities of cold disk gas into hot halo gas. Most TDGs form between two interacting gas rich disk galaxies (Kaviraj et al. 2012). If tidal streams and TDGs indicate that most external disk galaxies do not contain hot gas halos, then perhaps this indicates that the MW and/or the Local group is atypical.

A lack of hot halo gas in many late-type disk galaxies could have far-reaching consequences for disk galaxy evolution in general. Significant quantities of hot gas in a halo are a natural consequence of galaxy formation and evolution in Λ CDM (Courty et al. 2010), and a restocking of cold gas via cooling-out from a hot gas halo is required to

maintain star formation rates, reproduce observed metallicity gradients (Pilkington et al. 2012; Gibson et al. 2013), and produce realistic disk morphologies (Hambleton et al. 2011; Stinson et al. 2012). Our results may also have implications for the proposed TDG origin of the Local Group dwarf galaxies (Metz et al. 2009; Kroupa et al. 2010).

5 SUMMARY AND CONCLUSIONS

Tidal dwarf galaxies (TDGs) contain little or no dark matter. As such, they might be expected to be highly sensitive to their environment. In this study, we wish to understand the impact of ram pressure on TDGs. Ram pressure could arise from the motion of a TDG through the hot gaseous halos of its progenitor galaxies. Alternatively the ram pressure may arise if TDGs, which evade destruction by their progenitor galaxies, subsequently enter a group or galaxy cluster environment.

We submit TDG models, consisting of an exponential disk of gas and stars, to wind-tunnel ram pressure stripping tests. We conduct a parameter study, varying properties of the TDG models (such as mass, size, and gas fraction), and also varying the strength of the ram pressure.

We use a ‘toy’ ram pressure model, and wind tunnel tests to study the effects of ram pressure on TDGs. Although this approach is highly idealised, we emphasise that the mechanism behind our key result – the unbinding of stars – is primarily the removal of the potential provided by the gas. Disk acceleration by ram pressure drag can further enhance stellar losses, but only if the loss of the gas potential first perturbs the stars. By definition ram pressure stripping involves the removal of the gas. Therefore this study highlights the sensitivity of tidal dwarf galaxies to ram pressure.

Our key results may be summarised as follows.

(i) The lack of a dark matter halo makes TDGs very sensitive to ram pressure.

(ii) At radii in the TDG disk where the gas is ram pressure stripped, the stars are unbound. This causes the gas *and stellar* disk to be truncated. If all of the gas is stripped, our TDG models are entirely destroyed.

(iii) Ram pressure causes a drag force on TDGs that accelerates them. Acceleration enhances star losses beyond that which occur from the loss of the gas mass alone. Acceleration can also cause unbound stars to lie in a low surface brightness stellar stream that is uncorrelated with the stripped gas stream.

(iv) For weak ram pressures, truncation of the stellar disk causes the surface density profile to have a reduced effective radius. For strong ram pressure that quickly sweeps out the gas, the stars are unbound and form an expanding envelope. In this case the effective radius steadily grows with time, while the surface density decreases. The Sersic index is only weakly affected.

(v) The stellar dynamics of partially stripped TDG models provide dynamical masses that are within a factor of 2 of the real mass. However the stellar dynamics of TDG models that lose all their gas provide highly inflated dynamical masses – up to ~ 10 times the true mass.

TDGs are expected to contain little or no dark matter. Therefore they might be expected to be very sensitive to

their environment. This includes external tides from other galaxies or, as this study demonstrates, ram pressure. Those TDGs that survive these multiple survival hurdles, might be expected to have very different properties from those with which they originally formed. We suggest that the role of ram pressure in simulations that form TDGs be considered carefully. The strong response of TDGs (and presumably the tidal tails from which they formed) to ram pressure make them sensitive probes of their local environment, and may provide constraints on the hot gas content of interacting galaxies.

ACKNOWLEDGEMENTS

MF acknowledges support by FONDECYT grant 1095092 and FONDECYT grant 1130521, RS acknowledges support by FONDECYT grant 3120135, and GC acknowledges support by FONDECYT grant 3130480. YKS acknowledges support by FONDECYT grant 3130470. BKG acknowledges the support of the UK Science & Technology Facilities Council (ST/J001341/1), and the generous visitor support provided by FONDECYT and the Universidad de Concepcion.

REFERENCES

- Abadi M. G., Moore B., Bower R. G., 1999, MNRAS, 308, 947
 Barnes J. E., Hernquist L., 1992, Nature, 360, 715
 Beasley M. A., Cenarro A. J., Strader J., Brodie J. P., 2009, AJ, 137, 5146
 Beasley M. A., Strader J., Brodie J. P., Cenarro A. J., Geha M., 2006, AJ, 131, 814
 Bekki K., 2009, MNRAS, 399, 2221
 Blitz L., Robishaw T., 2000, ApJ, 541, 675
 Boquien M., Duc P.-A., Galliano F., Braine J., Lisenfeld U., Charmandaris V., Appleton P. N., 2010, AJ, 140, 2124
 Bournaud F., 2010, Advances in Astronomy, 2010
 Bournaud F., Duc P.-A., Amram P., Combes F., Gach J.-L., 2004, A&A, 425, 813
 Bournaud F., Duc P.-A., Brinks E., Boquien M., Amram P., Lisenfeld U., Koribalski B. S., Walter F., Charmandaris V., 2007, Science, 316, 1166
 Bournaud F., Duc P.-A., Emsellem E., 2008, MNRAS, 389, L8
 Bournaud F., Duc P.-A., Masset F., 2003, A&A, 411, L469
 Bournaud F., Jog C. J., Combes F., 2007, A&A, 476, 1179
 Braine J., Duc P.-A., Lisenfeld U., Charmandaris V., Vallejo O., Leon S., Brinks E., 2001, A&A, 378, 51
 Bregman J. N., Lloyd-Davies E. J., 2007, ApJ, 669, 990
 Brook C. B., Stinson G., Gibson B. K., Wadsley J., Quinn T., 2012, MNRAS, 424, 1275
 Caon N., Capaccioli M., D’Onofrio M., 1993, MNRAS, 265, 1013
 Connors T. W., Kawata D., Gibson B. K., 2006, MNRAS, 371, 108
 Courty S., Gibson B. K., Teyssier R., 2010, in Debatista V. P., Popescu C. C., eds, American Institute of Physics Conference Series Vol. 1240 of American Institute of Physics Conference Series, The Circum-Galactic Gas Around Cosmologically Simulated Disks. pp 131–134

- Crosthwaite L. P., Turner J. L., Ho P. T. P., 2000, *AJ*, 119, 1720
- Di Matteo P., Montuori M., Lehnert M. D., Combes F., Semelin B., 2011, in Carignan C., Combes F., Freeman K. C., eds, *IAU Symposium Vol. 277 of IAU Symposium, Gas Inflows, Star Formation and Metallicity Evolution in Galaxy Pairs*. pp 246–249
- D’Onghia E., Besla G., Cox T. J., Hernquist L., 2009, *Nature*, 460, 605
- Duc P.-A., 2012, *Birth, Life and Survival of Tidal Dwarf Galaxies*. p. 305
- Duc P.-A., Bournaud F., Masset F., 2004, *A&A*, 427, 803
- Duc P.-A., Braine J., Lisenfeld U., Brinks E., Boquien M., 2007, *A&A*, 475, 187
- Duc P.-A., Brinks E., Springel V., Pichardo B., Weilbacher P., Mirabel I. F., 2000, *AJ*, 120, 1238
- Duc P.-A., Mirabel I. F., 1994, *A&A*, 289, 83
- Duc P.-A., Mirabel I. F., 1998, *A&A*, 333, 813
- Elmegreen B. G., Kaufman M., Thomasson M., 1993, *ApJ*, 412, 90
- Evans N. W., Wilkinson M. I., Perrett K. M., Bridges T. J., 2003, *ApJ*, 583, 752
- Farouki R., Shapiro S. L., 1980, *ApJ*, 241, 928
- Feldmann R., Hooper D., Gnedin N. Y., 2013, *ApJ*, 763, 21
- Freeman K. C., 1970, *ApJ*, 160, 811
- Gatto A., Fraternali F., Read J. I., Marinacci F., Lux H., Walch S., 2013, *MNRAS*, 433, 2749
- Gavazzi G., Giovanelli R., Haynes M. P., Fabello S., Fumagalli M., Kent B. R., Koopmann R. A., Brosch N., Hoffman G. L., Salzer J. J., Boselli A., 2008, *HI content and other structural properties of galaxies in the Virgo cluster from the Arecibo Legacy Fast ALFA Survey*
- Gibson B. K., Pilkington K., Brook C. B., Stinson G. S., Bailin J., 2013, *A&A*, 554, A47
- Gingold R. A., Monaghan J. J., 1983, *MNRAS*, 204, 715
- Gupta A., Mathur S., Krongold Y., Nicastro F., Galeazzi M., 2012, *ApJL*, 756, L8
- Hambleton K. M., Gibson B. K., Brook C. B., Stinson G. S., Conselice C. J., Bailin J., Couchman H., Wadsley J., 2011, *MNRAS*, 418, 801
- Hancock M., Smith B. J., Struck C., Giroux M. L., Appleton P. N., Charmandaris V., Reach W. T., 2007, *AJ*, 133, 676
- Hernquist L., Katz N., 1989, *ApJS*, 70, 419
- Hibbard J. E., van der Hulst J. M., Barnes J. E., Rich R. M., 2001, *AJ*, 122, 2969
- Hibbard J. E., van Gorkom J. H., 1996, *AJ*, 111, 655
- Hibbard J. E., Yun M. S., 1999, *AJ*, 118, 162
- Hunsberger S. D., Charlton J. C., Zaritsky D., 1996, *ApJ*, 462, 50
- Hunter D., 1997, *PASP*, 109, 937
- Hunter D. A., Hunsberger S. D., Roye E. W., 2000, *ApJ*, 542, 137
- Iglesias-Páramo J., van Driel W., Duc P.-A., Papaderos P., Vilchez J. M., Cayatte V., Balkowski C., O’Neil K., Dickey J., Hernández H., Thuan T. X., 2003, *A&A*, 406, 453
- Katz N., 1991, *ApJ*, 368, 325
- Kaviraj S., Darg D., Lintott C., Schawinski K., Silk J., 2012, *MNRAS*, 419, 70
- Knebe A., Power C., Gill S. P. D., Gibson B. K., 2006, *MNRAS*, 368, 741
- Knierman K. A., Gallagher S. C., Charlton J. C., Hunsberger S. D., Whitmore B., Kundu A., Hibbard J. E., Zaritsky D., 2003, *AJ*, 126, 1227
- Koribalski B. S., López-Sánchez Á. R., 2009, *MNRAS*, 400, 1749
- Kroupa P., Famaey B., de Boer K. S., Dabringhausen J., Pawlowski M. S., Boily C. M., Jerjen H., Forbes D., Hensler G., Metz M., 2010, *A&A*, 523, A32+
- Lehner N., Zech W. F., Howk J. C., Savage B. D., 2011, *ApJ*, 727, 46
- Lianou S., Grebel E. K., Koch A., 2010, *A&A*, 521, A43
- Marcolini A., Brighenti F., D’Ercole A., 2003, *MNRAS*, 345, 1329
- Mayer L., 2005, in Jerjen H., Binggeli B., eds, *IAU Colloq. 198: Near-fields cosmology with dwarf elliptical galaxies The environment of dwarf spheroidal satellites; ram pressure, tides and external radiation fields*. pp 220–228
- Metz M., Kroupa P., Jerjen H., 2009, *MNRAS*, 394, 2223
- Mihos J. C., 2001, *ApJ*, 550, 94
- Muccione V., Ciotti L., 2004, *A&A*, 421, 583
- Mundell C. G., James P. A., Loiseau N., Schinnerer E., Forbes D. A., 2004, *ApJ*, 614, 648
- Mushotzky R., 2004, *Advances in Space Research*, 34, 2492
- Neff S. G., Thilker D. A., Seibert M., Gil de Paz A., Bianchi L., Schiminovich D., Martin D. C., Madore B. F., Rich R. M., Barlow T. A., Byun Y.-I., Donas J., Forster K., Friedman P. G., Heckman T. M., Jelinsky P. N., Lee Y.-W., Malina R. F., Milliard 2005, *ApJL*, 619, L91
- Paudel S. e., , 2013, *MNRAS*, in prep
- Peñarrubia J., Navarro J. F., McConnachie A. W., 2008, *Astronomische Nachrichten*, 329, 934
- Pilkington K., Few C. G., Gibson B. K., Calura F., Michel-Dansac L., Thacker R. J., Mollá M., Matteucci F., Rahimi A., Kawata D., Kobayashi C., Brook C. B., Stinson G. S., Couchman H. M. P., Bailin J., Wadsley J., 2012, *A&A*, 540, A56
- Pilkington K., Gibson B. K., Brook C. B., Calura F., Stinson G. S., Thacker R. J., Michel-Dansac L., Bailin J., Couchman H. M. P., Wadsley J., Quinn T. R., Maccio A., 2012, *MNRAS*, 425, 969
- Pilkington K., Gibson B. K., Calura F., Brooks A. M., Mayer L., Brook C. B., Stinson G. S., Thacker R. J., Few C. G., Cunnama D., Wadsley J., 2011, *MNRAS*, 417, 2891
- Puchwein E., Springel V., Sijacki D., Dolag K., 2010, *MNRAS*, 406, 936
- Putman M. E., Bland-Hawthorn J., Veilleux S., Gibson B. K., Freeman K. C., Maloney P. R., 2003, *ApJ*, 597, 948
- Putman M. E., Staveley-Smith L., Freeman K. C., Gibson B. K., Barnes D. G., 2003, *ApJ*, 586, 170
- Quilis V., Moore B., Bower R., 2000, *Science*, 288, 1617
- Recchi S., Theis C., Kroupa P., Hensler G., 2007, *A&A*, 470, L5
- Roediger E., Brügggen M., 2006, *MNRAS*, 369, 567
- Roediger E., Brügggen M., 2007, *MNRAS*, 380, 1399
- Rots A. H., Bosma A., van der Hulst J. M., Athanassoula E., Crane P. C., 1990, *AJ*, 100, 387
- Schulz S., Struck C., 2001, *MNRAS*, 328, 185
- Sembach K. R., Wakker B. P., Savage B. D., Richter P., Meade M., Shull J. M., Jenkins E. B., Sonneborn G., Moos H. W., 2003, *ApJS*, 146, 165
- Sheen Y.-K., Jeong H., Yi S. K., Ferreras I., Lotz J. M.,

- Olsen K. A. G., Dickinson M., Barnes S., Park J.-H., Ree C. H., Madore B. F., Barlow T. A., Conrow T., Foster K., Friendman P. G., Lee Y.-W., Martin D. C., Morrissey P., Neff S. G., Schiminovich D., 2009, *AJ*, 138, 1911
- Shlosman I., Noguchi M., 1993, *ApJ*, 414, 474
- Smith R., Fellhauer M., Assmann P., 2012, *MNRAS*, 420, 1990
- Smith R., Sánchez-Janssen R., Fellhauer M., Puzia T. H., Aguerri J. A. L., Farias J. P., 2013, *MNRAS*, 429, 1066
- Springel V., White S. D. M., 1999, *MNRAS*, 307, 162
- Stanimirović S., Dickey J. M., Krčo M., Brooks A. M., 2002, *ApJ*, 576, 773
- Stinson G. S., Brook C., Prochaska J. X., Hennawi J., Shen S., Wadsley J., Pontzen A., Couchman H. M. P., Quinn T., Macciò A. V., Gibson B. K., 2012, *MNRAS*, 425, 1270
- Struck C., Kaufman M., Brinks E., Thomasson M., Elmegreen B. G., Elmegreen D. M., 2005, *MNRAS*, 364, 69
- Tamburro D., Rix H., Leroy A. K., Mac Low M., Walter F., Kennicutt R. C., Brinks E., de Blok W. J. G., 2009, *AJ*, 137, 4424
- Temporin S., Weinberger R., Galaz G., Kerber F., 2003, *ApJ*, 587, 660
- Tielens A. G. G. M., 2010, *The Physics and Chemistry of the Interstellar Medium*
- Tonnesen S., Bryan G. L., 2009, *ApJ*, 694, 789
- Trentham N., Tully R. B., 2002, *MNRAS*, 335, 712
- Tripp T. M., Meiring J. D., Prochaska J. X., Willmer C. N. A., Howk J. C., Werk J. K., Jenkins E. B., Bowen D. V., Lehner N., Sembach K. R., Thom C., Tumlinson J., 2011, *Science*, 334, 952
- Tumlinson J., Werk J. K., Thom C., Meiring J. D., Prochaska J. X., Tripp T. M., O'Meara J. M., Okrochkov M., Sembach K. R., 2011, *ApJ*, 733, 111
- Vollmer B., Braine J., Pappalardo C., Hily-Blant P., 2008, *A&A*, 491, 455
- Vollmer B., Cayatte V., Balkowski C., Duschl W. J., 2001, *ApJ*, 561, 708
- Weilbacher P. M., Duc P.-A., Fritze-v. Alvensleben U., 2003, *A&A*, 397, 545
- Weiner B. J., Williams T. B., 1996, *AJ*, 111, 1156
- Wetzstein M., Naab T., Burkert A., 2007, *MNRAS*, 375, 805
- Williams P. R., 1998, PhD thesis, University of Cardiff
- Williams P. R., Churches D. K., Nelson A. H., 2004, *ApJ*, 607, 1
- Williams P. R., Nelson A. H., 2001, *A&A*, 374, 839
- Wolf J., Martinez G. D., Bullock J. S., Kaplinghat M., Geha M., Muñoz R. R., Simon J. D., Avedo F. F., 2010, *MNRAS*, 406, 1220
- Yun M. S., Ho P. T. P., Lo K. Y., 1994, *Nature*, 372, 530
- Zabludoff A. I., Mulchaey J. S., 1998, *ApJ*, 496, 39